Report

Cell Reports

A Small-Molecule Screen for Enhanced Homing of Systemically Infused Cells

Graphical Abstract

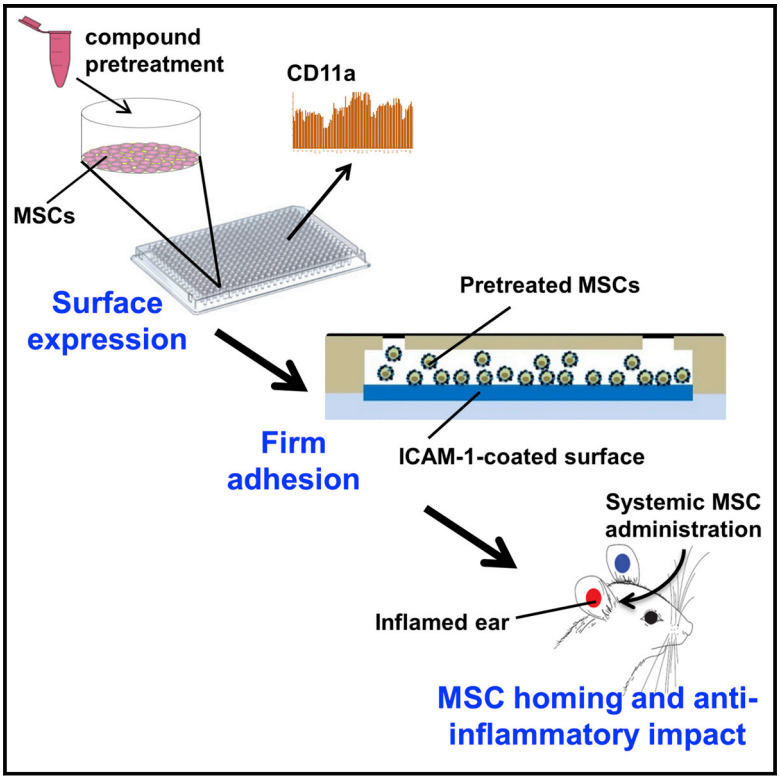

Authors

Oren Levy, Luke J. Mortensen, ..., Charles P. Lin, Jeffrey M. Karp

Correspondence

lin@helix.mgh.harvard.edu (C.P.L.), jeffkarp.bwh@gmail.com (J.M.K.)

In Brief

Levy et al. developed a multi-step screening process to identify small molecules that improve targeting of systemically infused mesenchymal stem cells to sites of inflammation, resulting in a heightened anti-inflammatory response. This multi-step screening platform may significantly improve clinical outcomes of cell-based therapies.

Highlights

- Compounds were screened to maximize MSC surface expression of ICAM-1-binding ligands
- Ro-31-8425, a kinase inhibitor, was identified to enhance cell adhesion under flow
- Preconditioning of MSCs enabled their targeting to a distant inflamed tissue
- Improved therapeutic anti-inflammatory response was also achieved

Levy et al., 2015, Cell Reports *10*, 1261–1268
March 3, 2015
http://dx.doi.org/10.1016/j.celrep.2015.01.057

Cell Reports
Report

A Small-Molecule Screen for Enhanced Homing of Systemically Infused Cells

Oren Levy,[1,2,3,7] Luke J. Mortensen,[2,4,7,8] Gerald Boquet,[5,7] Zhixiang Tong,[1,2,3] Christelle Perrault,[5] Brigitte Benhamou,[5] Jidong Zhang,[5] Tara Stratton,[2,4] Edward Han,[1,2,3] Helia Safaee,[1,2,3] Juliet Musabeyezu,[1,2,3] Zijiang Yang,[1,2,3] Marie-Christine Multon,[5] Jonathan Rothblatt,[6] Jean-Francois Deleuze,[5,9] Charles P. Lin,[2,4,*] and Jeffrey M. Karp[1,2,3,*]

[1]Division of Biomedical Engineering, Department of Medicine, Center for Regenerative Therapeutics, Brigham and Women's Hospital, Harvard Medical School, Cambridge, MA 02139, USA
[2]Harvard Stem Cell Institute, Cambridge, MA 02139, USA
[3]Harvard-MIT Division of Health Sciences and Technology, Cambridge, MA 02139, USA
[4]Wellman Center for Photomedicine and Center for Systems Biology, Massachusetts General Hospital, Harvard Medical School, Boston, MA 02114, USA
[5]Sanofi R&D, Centre de Recherche Vitry-Alfortville, 13 quai Jules Guesde, 94403 Vitry-sur-Seine, France
[6]Sanofi R&D, 270 Albany Street, Cambridge, MA 02139, USA
[7]Co-first author
[8]Present address: Regenerative Bioscience Center, Rhodes Center for ADS, and College of Engineering, University of Georgia, Athens, GA 30602, USA
[9]Present address: Centre National de Génotypage, CEA Institut de Génomique, 2 rue Gaston Crémieux, CP5721, 91057 Evry, France; and Centre d'Etudes du Polymorphisme Humain, Fondation Jean Dausset, 27 rue Juliette Dodu, 75010 Paris, France
*Correspondence: lin@helix.mgh.harvard.edu (C.P.L.), jeffkarp.bwh@gmail.com (J.M.K.)
http://dx.doi.org/10.1016/j.celrep.2015.01.057

SUMMARY

Poor homing of systemically infused cells to disease sites may limit the success of exogenous cell-based therapy. In this study, we screened 9,000 signal-transduction modulators to identify hits that increase mesenchymal stromal cell (MSC) surface expression of homing ligands that bind to intercellular adhesion molecule 1 (ICAM-1), such as CD11a. Pretreatment of MSCs with Ro-31-8425, an identified hit from this screen, increased MSC firm adhesion to an ICAM-1-coated substrate in vitro and enabled targeted delivery of systemically administered MSCs to inflamed sites in vivo in a CD11a- (and other ICAM-1-binding domains)-dependent manner. This resulted in a heightened anti-inflammatory response. This represents a new strategy for engineering cell homing to enhance therapeutic efficacy and validates CD11a and ICAM-1 as potential targets. Altogether, this multi-step screening process may significantly improve clinical outcomes of cell-based therapies.

INTRODUCTION

While exogenous cell therapy is a promising approach for treating several tragic diseases (de Girolamo et al., 2013), a major challenge is that the majority of cell types exhibit poor homing to disease sites (Karp and Leng Teo, 2009). Herein, we report for the first time a multi-step process that includes a medium-throughput screen to detect small molecules that improve targeting of systemically infused mesenchymal stromal cells (MSCs) to sites of inflammation. MSCs are promising candidates for cell therapy given their pleotropic properties (Hoogduijn et al., 2010; Prockop and Oh, 2012). Specifically, MSCs can be readily isolated from bone marrow, fat, and other adult tissues, thus avoiding ethical issues, and can be expanded under ex vivo conditions to obtain a sufficient quantity for transplantation (Dominici et al., 2006). They are considered immune evasive (Ankrum et al., 2014), and their multi-lineage differentiation potential as well as potent immunomodulatory properties prompted their exploration in over 420 clinical trials as potential treatment for many tragic diseases (https://clinicaltrials.gov, December 2014). While results from preclinical animal studies have been encouraging and hundreds of millions of allogeneic MSCs can be safely administered systemically to patients, clinical trials have produced mixed results and the translational potential of MSCs has not yet been realized (Ankrum and Karp, 2010; François and Galipeau, 2012). The majority of clinical trials involve systemic infusion of MSCs, yet MSCs exhibit poor homing to diseased or damaged tissues (Ankrum and Karp, 2010). Key ligands of the classical cell-homing cascade that mediate dynamic cell interactions with activated endothelium are minimally expressed by MSCs or lost during in vitro expansion (Rombouts and Ploemacher, 2003; Sarkar et al., 2011). Modifying MSCs with homing ligands via DNA transfection and different surface modifications improves their targeting to diseased sites (Enoki et al., 2010; Sackstein et al., 2008; Sarkar et al., 2011). However, such approaches could be challenging to scale up in a cost-effective manner and include safety concerns in the case of viral modifications. Manipulation of signaling pathways via small-molecule pretreatment is a simple, cost-effective, and scalable approach to improve control over cell fate. Furthermore, as small-molecule pretreatment only transiently activates signal transduction pathways, and because the small molecule is

not directly delivered to patients, safety is another advantage. Although several high-throughput screens of bioactive compounds have been performed to identify molecules that modulate cellular processes relevant to cell therapy, few have been translated into promising in vivo preclinical results (Cutler et al., 2013). For instance, a zebrafish high-throughput screen yielded a stabilized prostaglandin that improves hematopoietic stem cell homeostasis and is currently being examined in a phase 2 clinical trial (Cutler et al., 2013). In this study, we describe a screening platform to identify small molecules that augment MSC therapeutic potential via increased adhesion to intercellular adhesion molecule 1 (ICAM-1). Ro-31-8425, identified in this screen to upregulate CD11a expression, enhanced MSC firm adhesion to ICAM-1, promoted targeting of systemically infused MSCs to sites of inflammation, and boosted their therapeutic impact.

RESULTS

A Medium-Throughput Screen of 9,000 Compounds Identified Ro-31-8425, a Kinase Inhibitor that Upregulates CD11a Expression on the MSC Surface

In this study, we aimed to increase MSC surface expression of key homing ligands via small-molecule pretreatment to improve homing of systemically administered MSCs to sites of inflammation (Graphical Abstract). Integrins, such as vascular cell adhesion molecule 1, were previously implicated in MSC homing (Teo et al., 2012), and engineering MSCs (via antibody [Ab] coating or viral DNA transfection) to overexpress integrins can promote targeting of systemically infused MSCs to disease sites (Ko et al., 2010; Kumar and Ponnazhagan, 2007). We focused on surface expression of ligands that bind ICAM-1, such as CD11a, otherwise known as integrin alpha L (ITGAL). CD11a combines with integrin beta 2 (CD18) to create lymphocyte function-associated antigen-1 (LFA-1), which serves a central role in mediating leukocyte firm adhesion, an important step in the inflammatory leukocyte-homing cascade (Luster et al., 2005).

For detection of CD11a on cell surface, we used a PE-CY5-conjugated anti-CD11a Ab. As shown in Figure 1A, CD11a is highly expressed on promyelocytic leukemia cells (HL-60, positive control), but not on the surface of culture-expanded MSCs. This anti-CD11a Ab was then used in a medium-throughput screening of 9,000 compounds, including a proprietary collection of 2,500 signaling pathway modulators, to identify candidate molecules that increase expression of CD11a on the MSC surface. Cells were pretreated with each small molecule (24 hr), followed by incubation with a PE-CY5-conjugated anti-CD11a Ab to detect its expression on the MSC surface (Figure 1B; Experimental Procedures). Our screen identified six compounds that significantly increased the expression of CD11a on the MSC surface. The most potent molecule emerging from this screen was the kinase inhibitor Ro-31-8425 (CAS #131848-97-0) (Figure S1A), previously shown to have an inhibitory effect on PKC (Muid et al., 1991). As shown Figure 1C, Ro-31-8425 induced a dose-dependent increase in the percentage of CD11a-positive MSCs as quantified by mass cytometry (CyTOF; see Experimental Procedures). Evaluation of MSC viability demonstrated that Ro-31-8425 did not significantly compromise cell viability at concentrations of 0.25–4 μM following a 24 hr pretreatment (Figure S1B; Ro-31-8425 exhibited toxicity only at >4 μM post-72 hr pretreatment of MSCs) and did not upregulate mRNA levels of CD18 (integrin β2, known to pair with CD11a to form LFA-1; Figure S1C). Of note, Ro-31-8425 did not substantially alter the MSC secretome (Figure S1D; out of 48 secreted factors tested via Ab-based multiplex assays, only 3 showed statistically significant changes in response to Ro-31-8425 pretreatment). As shown in Figure 1C, CyTOF analysis demonstrated that Ro-31-8425 treatment at 3 μM triggered a significant increase in the percentage of MSCs exhibiting surface expression of CD11a compared to virtually no $CD11a^+$ MSCs under control conditions. The percentage of $CD11a^+$ MSCs in response to Ro-31-8425 (3 μM for 24 hr) was stable for at least 4 days (Figure S2A; similar pretreatment conditions were used for all subsequent experiments). As shown in Figure 1D, RT-PCR analysis revealed that Ro-31-8425 also significantly increased CD11a mRNA levels in MSCs, with peak levels observed 14 hr post-incubation, indicating an impact of Ro-31-8425 pretreatment on MSC CD11a also at the transcriptional level. Importantly, Ro-31-8425 increased CD11a expression to a similar magnitude on MSCs from multiple donors (Figure S2B). Establishing a donor-independent response is critical for successful clinical translation of exogenous cell therapy.

Pretreatment of MSCs with Ro-31-8425 Enhanced MSC Firm Adhesion to an ICAM-1-Coated Surface under Dynamic Flow Conditions

Considering the key role of CD11a in mediating leukocyte firm adhesion, we next assessed the effect of the identified CD11a-upregulating hits on MSC firm adhesion, which is part of the leukocyte adhesion cascade and is also governed by CD11a (Luster et al., 2005). CD11a is known to mediate leukocyte firm adhesion with endothelial cells via interaction with intercellular adhesion molecules, and specifically ICAM-1 (Bhatia et al., 2003; Luster et al., 2005). Therefore, we tested firm adhesion of pretreated MSCs to ICAM-1, which is upregulated on the endothelial surface at sites of inflammation and is involved in leukocyte recruitment during inflammation (Kim et al., 2001; Luster et al., 2005; Wong and Dorovini-Zis, 1992). MSCs were incubated with each of the positive hits, and then subjected to a firm adhesion assay under physiologically relevant shear flow using a multiwell plate microfluidic system (Experimental Procedures) (Levy et al., 2013a). Pretreatment with Ro-31-8425, which upregulated CD11a expression, induced a >3-fold increase in MSC firm adhesion to an ICAM-1-coated substrate compared to control, vehicle-treated MSCs (Figures 2Ai and 2Aii). As depicted in Figure 2Aiii, Ro-31-8425 pretreatment induced ICAM-1 firm adhesion of a new MSC sub-population comprising 68% of the entire population, out of which ~7% are $CD11a^+$ (Figure 1C) and the rest (61%) express other active ICAM-1-binding domains/adhesion molecules. Ro-31-8425 also increased MSC firm adhesion to E-selectin-coated surface, further indicating that Ro-31-8425 induces upregulation/activation of additional adhesion molecules on the MSC surface (Figure S3C). In contrast, the PKC inhibitor ruboxistaurin (Joy et al., 2005; Tang et al., 2008), which

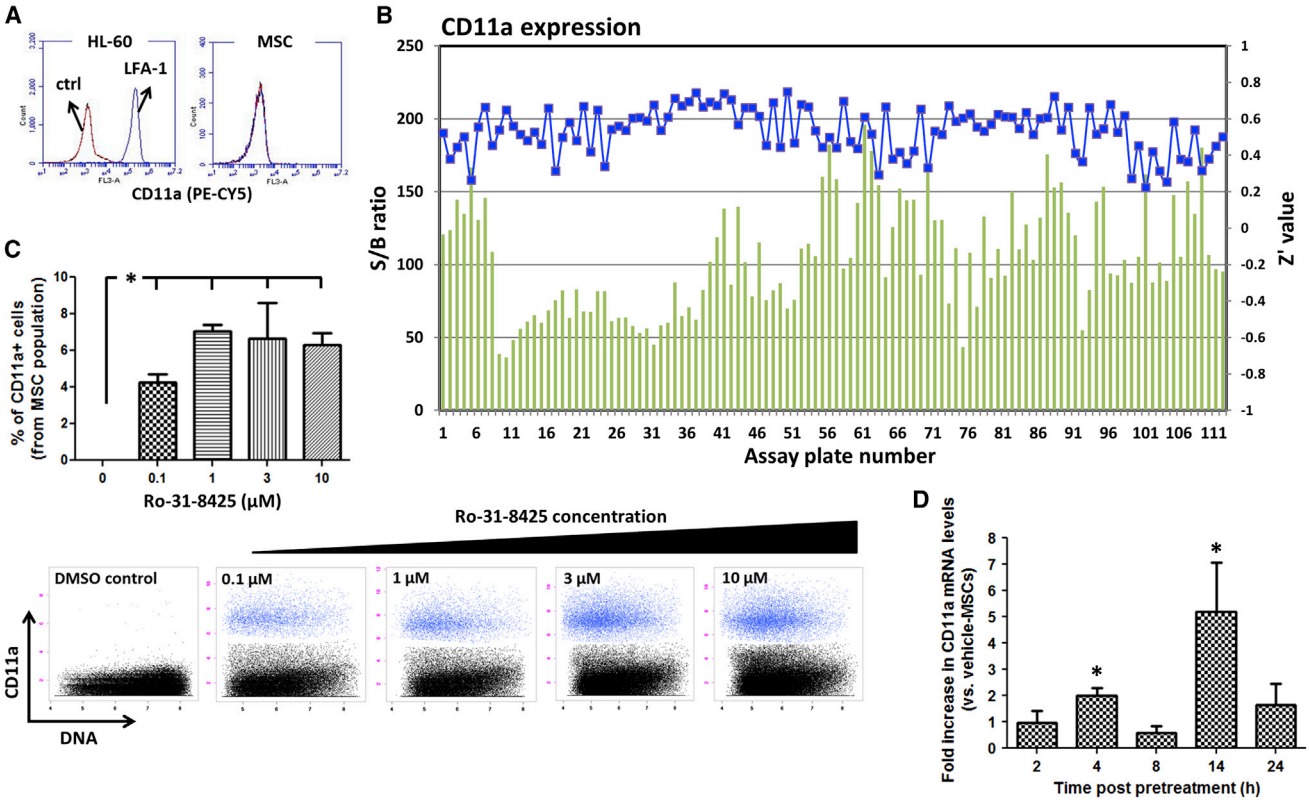

Figure 1. A Medium-Throughput Screen Identified Ro-31-8425, a Kinase Inhibitor that Upregulates CD11a Expression on the MSC Surface

(A) Native MSCs lack surface expression of CD11a. Cells (HL-60 or MSCs) were incubated with PE-CY5-CD11a Ab and analyzed by flow cytometry (representative data from n = 3 independent experiments).

(B) Global screening data obtained from the medium-throughput screening to identify compounds that upregulate CD11a expression on the MSC surface (9,000 compounds in 112 384-well assay plates were screened; green bars, S/B [signal/background ratio]; blue curve, Z′ values). See also Experimental Procedures.

(C) A dose-dependent increase in the percentage of CD11a$^+$ MSCs in response to Ro-31-8425 pretreatment. MSCs were pretreated with DMSO vehicle control (0.1%) or Ro-31-8425 (0.1, 1, 3 and 10 μM) for 24 hr and CD11a expression levels were assessed by CyTOF analysis. Error bars represent SD (n = 3; blue dots, CD11a$^+$ MSCs; black dots, CD11a$^-$ MSCs). *p < 0.05 versus DMSO-treated control MSCs (Tukey's HSD test).

(D) CD11a mRNA levels in response to Ro-31-8425 pretreatment as analyzed by RT-PCR. MSCs were pretreated with Ro-31-8425 (3 μM), and CD11a mRNA levels were analyzed at indicated times post pretreatment. Error bars represent SD (n = 3). *p < 0.05 versus DMSO-treated control MSCs (Tukey's HSD test).

also belongs to the chemical family of bisindoles (Figure S3A) but did not increase MSC CD11a expression in our screen (Figure S3B), did not improve MSC firm adhesion to ICAM-1-coated substrates (Figure 2A).

To explore the possible involvement of CD11a in mediating pretreated MSC firm adhesion to an ICAM-1-coated surface, we performed Ab blocking experiments (Experimental Procedures). As shown in Figure 2B, incubating with CD11a-blocking Ab significantly reduced Ro-31-8425-pretreated MSC firm adhesion to ICAM-1-coated surface (a reduction from ~90% of adhered cells to 50% following CD11a blocking). These data suggest that CD11a, which was upregulated in response to Ro-31-8425 pretreatment, is involved in mediating the increased MSC firm adhesion to ICAM-1. However, CD11a blocking did not fully abolish Ro-31-8425-pretreated MSC firm adhesion to control untreated MSC levels, further suggesting that other ICAM-1-binding ligands are also involved in mediating the increased firm adhesion of Ro-31-8425-treated MSCs to ICAM-1.

Ro-31-8425-Preconditioned MSCs Home Efficiently to Inflamed Sites and Exhibit a Potent Anti-inflammatory Response

Compounds that significantly increased MSC firm adhesion to ICAM-1 in vitro were then tested in vivo for their ability to promote targeting of systemically administered MSCs to a distant site of inflammation. In our murine model, one ear pinna was injected with lipopolysaccharide (LPS) to induce local inflammation, while the other received a saline injection (Experimental Procedures). This model was previously established to evaluate several MSC bioengineering strategies (Levy et al., 2013b; Sarkar et al., 2011) and has recently been modified to maximize sensitivity (Mortensen et al., 2013). Briefly, compound-treated and vehicle MSCs (stained with different membrane tracker dyes and mixed at 1:1 ratio) were systemically infused into mice, and cell homing to the inflamed and control ears was imaged 24 hr later using intravital microscopy (Figure 3A; Experimental Procedures). Pretreatment with Ro-31-8425 significantly improved MSC homing to skin in the inflamed ear upon systemic

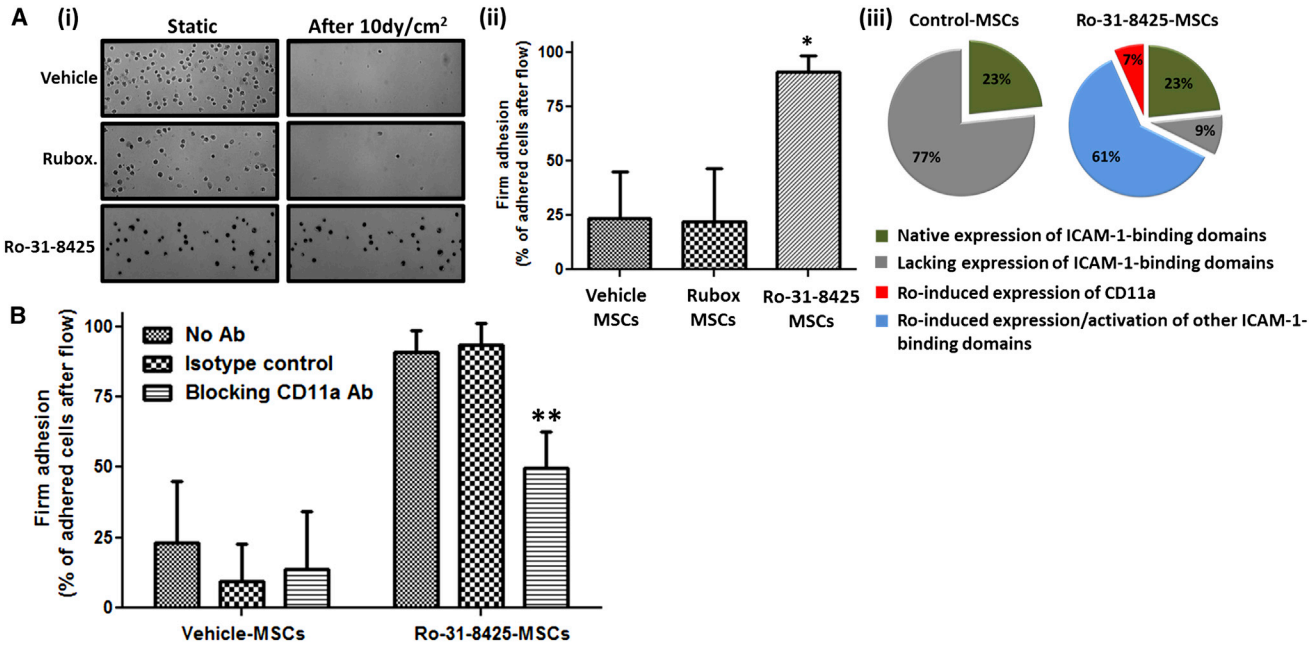

Figure 2. Upregulation of CD11a, in Response to Pretreatment with Ro-31-8425, Increases MSC Firm Adhesion to an ICAM-1-Coated Surface In Vitro

(Ai) MSC firm adhesion to an ICAM-1-coated surface following pretreatment with ruboxistaurin (Rubox) or Ro-31-8425 (3 μM for 24 hr, 10× magnification).

(Aii) Quantification of MSC firm adhesion to an ICAM-1 surface in response to pretreatment with ruboxistaurin and Ro-31-8425. Error bars represent SD (n = 3). Statistically significant difference versus vehicle-treated control is denoted by *$p < 0.05$ (Tukey's HSD test).

(Aiii) A pie chart of the percent distribution of MSC population that express active ICAM-1 binding domains following Ro-31-8425 pretreatment.

(B) Ab blocking experiments demonstrate a significant involvement of CD11a in the increased firm adhesion of Ro-31-8425-treated MSCs to the ICAM-1 surface. Error bars represent SD (n = 3). Statistically significant difference versus no Ab control and versus isotype control is denoted by *$p < 0.05$ (Tukey's HSD test).

administration, with an average of 45.2 ± 8.6 cells/mm^2 for vehicle-MSCs and 78.5 ± 15.9 cells/mm^2 for Ro-31-8425-MSCs (69.3 ± 11.3% increase compared to vehicle-treated MSCs). These data demonstrate a strong relationship among surface expression of CD11a, ICAM-1 firm adhesion, and homing of systemically transplanted MSCs to sites of inflammation.

Furthermore, when CD11a was blocked on Ro-31-8425-pretreated MSCs prior to systemic infusion, their enhanced homing response to the site of inflammation was reversed, dropping from 70% to less than 10% increased homing versus vehicle-treated MSCs (Figure 3B). These results further implicate CD11a and other ICAM-1 binding domains that mediate the enhanced homing response of systemically infused Ro-31-8425-pretreated MSCs to sites of inflammation. We then sought to assess the ability of Ro-31-8425-pretreated MSCs, which exhibited increased homing to the inflamed ear, to alleviate the severity of LPS-induced local inflammation. To evaluate ear inflammation, ear thickness and local levels of the pro-inflammatory cytokine tumor necrosis factor alpha (TNF-α) in mice ears were measured 24 hr post-administration of either vehicle or Ro-31-8425-pretreated MSCs (Experimental Procedures). As shown in Figure 3C, while mice treated with vehicle control MSCs exhibited a small reduction in ear thickness (6.3 ± 5.2 μm reduction compared to no MSC treatment), MSCs pretreated with Ro-31-8425 exhibited a greater than 3-fold effect in reducing ear swelling (20.0 ± 5.3 μm reduction). LPS-induced inflammation resulted not only in ear swelling but also in a significant increase in local levels of the pro-inflammatory cytokine TNF-α in the inflamed ear compared to the saline-treated ear (4.5- ± 1.3-fold TNF-α increase in the inflamed ear versus control ear; Figure 3D). Consistent with the cell delivery and ear thickness data, the increased TNF-α levels in the inflamed ear were significantly reduced (~50%) by administration of Ro-31-8425-treated MSCs, whereas vehicle-treated MSCs did not impact TNF-α levels (Figure 3D). Taken together, these results show that systemic infusion of Ro-31-8425-pretreated MSCs, which display CD11a and other ICAM-1 binding domains, increased homing to inflamed tissues and also results in improved anti-inflammatory therapeutic effect.

DISCUSSION

Our multi-step screening process identified small molecules that increased expression/activation of ICAM-1-binding ligands, such as CD11a, on the MSC surface, enhanced MSC firm adhesion to an ICAM-1-coated substrate, and also promoted MSC homing to sites of inflammation following systemic administration, resulting in an improved anti-inflammatory response. Our findings are supported by a number of previous approaches that enhanced MSC therapeutic impact via improved homing to disease sites (Enoki et al., 2010; Ko et al., 2010). Recently, we have shown that mRNA-induced expression of

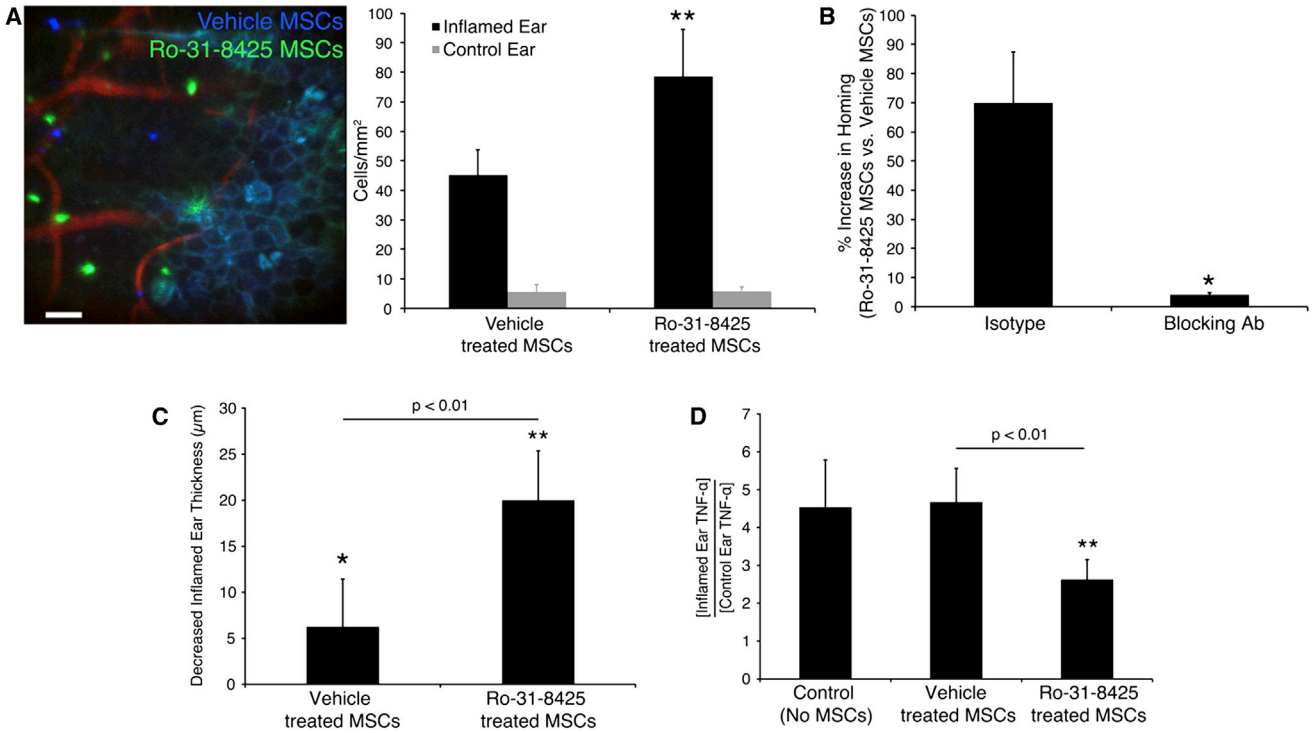

Figure 3. Ro-31-8425-Pretreated MSCs Exhibit Increased Homing to Inflamed Sites and an Improved Anti-Inflammatory Impact following Systemic Administration

(A) Homing of systemically infused MSCs to LPS-induced inflamed mouse ears was assessed 24 hr following cell infusion. An example 2D projection of a 3D image stack (scale bar, 50 μm) demonstrates homing to the inflamed ear of Ro-31-8425-pretreated MSCs (green cells) compared to vehicle-treated MSCs (blue cells). MSCs are found in the vascularized region of the skin (left side of image), with the skin surface exhibiting autofluorescence in multiple channels and a characteristic tiled pattern (right side of image). Ro-31-8425 pretreatment significantly promoted MSC homing versus the vehicle-treated control cells. Error bars represent SD (**$p < 0.01$, Tukey's HSD test; n = 8 mice).

(B) For Ab blocking experiments, Ro-31-8425 or vehicle-pretreated MSCs were washed and incubated for 30 min with mouse anti-human CD11a (clone TS1/22) or mouse IgG1 isotype control prior to staining with the Vybrant dyes and retro-orbital infusion as described above. Ab blocking experiments demonstrate involvement of CD11a and other ICAM-1 binding domains in the increased homing response of systemically infused Ro-31-8425-treated MSCs to the inflamed ear. CD11a-blocked or Ab isotype control-incubated Ro-31-8425-pretreted MSCs were co-injected systemically with vehicle MSCs (1:1 ratio), and the homing response to inflamed ear was assessed via intravital microscopy. Error bars represent SD (statistically significant difference versus Ab isotype control is denoted by *$p < 0.05$ [Tukey's HSD test]; n = 5 mice per group).

(C) Ro-31-8425-treated MSCs displayed a superior effect in reducing swollen ear thickness of the inflamed ear compared to native MSCs. Error bars represent SD (*$p < 0.05$, **$p < 0.01$, Tukey's HSD test; n = 8 mice).

(D) MSCs treated with Ro-31-8425 significantly reduced the TNF-α level in the inflamed ear compared to the control ear. Error bars represent SD (**$p < 0.01$, Tukey's HSD test; n = 6 mice).

SLeX/PSGL-1 (rolling ligands) resulted in a transient improvement of only 30% in MSC homing in the same local inflammation model and yielded a limited anti-inflammatory impact compared to untreated MSCs (Levy et al., 2013b). In this system, targeted SLeX/PSGL-1 MSCs required simultaneous transfection with interleukin-10 (IL-10) mRNA to achieve a functional anti-inflammatory effect (Levy et al., 2013b). Ro-31-8425 pretreatment induced a ~70% increase in MSC delivery to an inflamed site (via increased firm adhesion), which was reversed when cells were blocked with a CD11a antibody, implicating CD11a and other ICAM-1 binding domains in mediating the increased homing response of MSCs to sites of inflammation. CD11a antibody blocking also significantly inhibited MSC firm adhesion to ICAM-1 in vitro, though to a lesser extent (~50% inhibition), indicating that the antibody blocking in vivo may have also blocked MSC interaction with additional ligands on the inflamed endothelium due to steric interference. Interestingly, the in vitro ICAM-1 firm adhesion data, demonstrating a new ICAM-1-binding MSC sub-population (68% of the entire population) in response to Ro-31-8425 (composed of 7% $CD11a^+$ MSCs and an additional sub-population of 61% expressing other active ICAM-1-binding domains; Figure 2Aiii) correlates with the in vivo data of an ~70% increase in MSC homing to inflamed sites in response to Ro-31-8425 (Figure 3A). It is plausible that via modulation of key signaling pathways, Ro-31-8425 triggers firm adhesion to ICAM-1 (as well as to E-selectin) by inducing a slight upregulation (or conformational activation) of multiple adhesion molecules on the MSC surface, resulting in a broad and coordinated adhesion response. The improvement in MSC anti-inflammatory impact commensurate

with the enhanced homing response demonstrated herein suggests that upregulation of firm adhesion ligands, and specifically utilization of the ICAM-1 axis, is an attractive target to improve the efficacy of cell-based therapies.

The most promising small molecule identified in our study was the kinase inhibitor Ro-31-8425, previously demonstrated as a PKC inhibitor (Muid et al., 1991). Interestingly, PKC activation was shown to stimulate adhesion-mediated MSC retention in infarcted myocardium upon local administration by activation of focal adhesion kinase (Song et al., 2013). In our screen, we found that ruboxistaurin, a bis-indole that is chemically related to Ro-31-8425, as well as other PKC inhibitors, did not elicit CD11a expression on MSCs (Figure S3B) and also did not increase MSC firm adhesion to ICAM-1 (Figure 2A). This implies that the Ro-31-8425-induced increase in RNA levels and surface expression of CD11a, MSC firm adhesion to ICAM-1, and systemic targeting of MSCs to an inflamed site were not PKC dependent and potentially involve other kinases that may be targeted by Ro-31-8425, such as Rsk2, GSK-3β, and CDK2 (Brehmer et al., 2004). This finding should stimulate further research to better understand involvement of signal-transduction pathways in cell homing to sites of inflammation. Furthermore, correlating cell-surface adhesion receptor expression to in vitro and in vivo adhesion, and to a therapeutic response, should enable further improvements for exogenous cell therapy, in which targeting cells to diseased or damaged tissues is highly important. The endothelial receptor expression on vessels in specific tissues is well characterized, providing zip codes that can be used to help identify new hits to enable delivery of cells to specific tissues. Hence, small-molecule pretreatment can potentially serve as an effective methodology to target cells to virtually any tissue. Overall, the multi-step screening process described herein should provide an opportunity to significantly enhance the clinical efficacy of cell-based therapy.

EXPERIMENTAL PROCEDURES

Cell Culture and Compound Pretreatment

MSCs were purchased from Lonza (donors used were 7F3915, 318006, and 351482) and expanded in mesenchymal stem cell growth medium (MSCGM) (Lonza). Cells were kept at 37°C with 5% CO_2, and media were changed every 3 days. Cells were passaged using 1% trypsin-EDTA solution. MSCs at passage 3–7 were used for all experiments. HL-60 cells were purchased from ATCC and seeded in Iscove's modified Dulbecco's medium/GlutaMax containing 20% fetal bovine serum (Life Technologies).

Medium-Throughput Screen

MSCs were seeded on 384-well plates at 3,000 cells per well in MSCGM medium. Following an overnight incubation, cells were pretreated with a low (0.1 μM) and high (3 μM) concentration of the compounds for 24 hr (a total of 9,000 compounds were tested in 112 assay plates). Cells were washed and then incubated for 1 hr with PE-CY5-conjugated anti-CD11a monoclonal Ab (clone HI111, BD Biosciences). Expression of CD11a at the cell surface was detected using the Acumen Explorer, a laser-scanning fluorescence microplate cytometer. Positive compounds were counter-screened for their auto-fluorescence by measuring the signal in the absence of Ab. Shown in Figure 1B is the global screening data. For further details, including signal/background ratio (green columns) and the Z′-factor (blue curve) calculations, see Supplemental Experimental Procedures.

Cell Viability Assay

Pre-confluent MSCs were incubated with Ro-31-8425 at the indicated concentrations for 24 hr or 72 hr, and cell viability was assessed via an XTT assay according to manufacturer's instructions (ATCC).

Secretomic Analysis of Pretreated MSCs

MSCs (7F3915 or 318006) were seeded at 25,000 cells/well in a 12-well plate. 24 hr later, cells were treated with Ro-31-8425 (3 μM) or 0.1% DMSO (control). Following 24 hr of treatment, secretomic samples were collected, centrifuged, and frozen. MSC secretomes were assayed for the presence of cytokines, chemokines, and growth factors using Bio-plex human 21-plex and 27-plex immunoassay kits (Bio-Rad), according to the manufacturer's instructions. The 27-plex and 21-plex panels consisted of the following analytes: IL-1α, IL-1β, IL-1Rα, IL-2, IL-3, IL-4, IL-5, IL-6, IL-7, IL-8, IL-9, IL-10, IL-12p40, IL-12p70, IL-13, IL-15, IL-17, IL-18, CTACK, GROα, HGF, IFN-α2, LIF, MCP-1, MCP-3, MIF, MIG, β-NGF, SCF, SCGF-β, SDF-1α, TNF-α, TNF-β, TRAIL, Eotaxin, FGF-2, G-CSF, GM-CSF, IFN-γ, IP-10, MIP-1α, PDGF-bb, RANTES, and VEGF. A standard range of 0.2–3,200 pg/ml was used. Samples and controls were run in triplicate, and standards and blanks in duplicate (three independent experiments were performed for each donor).

mRNA Analysis of CD11a and CD18

mRNA levels of CD11a in response to Ro-31-8425 pretreatment of MSCs were analyzed by qPCR. Specifically, MSCs were treated with Ro-31-8425 (3 μM) or vehicle control (0.1% DMSO) for 2 hr, 4 hr, 8 hr, 14 hr, or 24 hr. Cells were then trypsinized, washed with ice-cold PBS, and pelleted (500 × *g* for 5 min at 4°C) at during the treatment and immediately stored at −80°C. RNA extraction was then performed as previously described (Tong et al., 2013), followed by a qPCR reaction using the following primers: for CD11α: 5′-CAGGCTAT TTGGGTTACACCG-3′ (sense); 5′-CCATGTGCTGGTATCGAGGG-3′ (anti-sense); for CD18: 5′-TGCGTCCTCTCTCAGGAGTG-3′ (sense); 5′-GGTCCAT GATGTCGTCAGCC-3′ (anti-sense). See also Supplemental Experimental Procedures.

CyTOF Analysis for Assessing CD11a Expression Levels

To further confirm the screening results, the surface expression of CD11a was also examined by time-of-flight mass cytometry (CyTOF2, DVS Sciences) (Newell et al., 2013). This approach, which uses metal-conjugated antibodies for detection of target proteins, was used to accurately assess CD11a expression levels on MSCs (using anti-human Nd142-labeled CD11a antibody, clone HI111) in response to Ro-31-8425, while minimizing any potential interference by the auto-fluorescent properties of this compound. MSCs were treated with Ro-31-8425 as indicated and sample preparation was performed per manufacturer's instructions. CyTOF data were analyzed with Cytobank online data analysis platform (https://www.cytobank.org/). See also Supplemental Experimental Procedures.

ICAM-1 and E-selectin Firm Adhesion Assay

Cell adhesion experiments were performed using Bioflux1000 (FluxionBio), allowing accurate control over shear flow (Levy et al., 2013a). A special 48-well plate was used, in which a microfluidic channel (350 ± 70 μm) connects each pair of adjacent wells (termed inlet and outlet wells). The plate was placed under vacuum and the channels were coated from the inlet with recombinant human ICAM-1 (5 μg/ml) or E-selectin (5 μg/ml) Fc chimeras and incubated at 37°C for 1 hr. Prior to introducing the cells into the channel, a wash with PBS −/− from the outlet well was performed for 5 min. Compound-pretreated MSCs were introduced into the channel, followed by an attachment period of 2 min (no flow applied during the attachment period). Attached cells were then subjected to increasing shear flow, ranging from 0.25 dynes/cm^2 for up to 10 dynes/cm^2. Images were acquired using the Montage software and cell adhesion to the ICAM-1-coated channels following subjection to shear flow was examined.

Ab Blocking Experiments

MSCs pretreated as indicated were detached, washed, and incubated for 30 min with a mouse anti-human CD11a-blocking Ab (clone: TS1/22) or a mouse IgG1 isotype control. Cells were then introduced into the microfluidic

channel and subjected to a firm adhesion assay on ICAM-1-coated channels.

Cell Staining for In Vivo Tracking

To track MSCs in vivo, cells were stained with lipophilic membrane dyes with emission wavelengths in the red (DiI) or far red (DiD) (Invitrogen), with the dye pair selected based on previous work (Mortensen et al., 2013). MSCs (10^6 cells/ml) were incubated with 10 μM DiI or 10 μM DiD in PBS + 0.1% BSA for 20 min at 37°C. MSCs were then washed twice in PBS and mixed in equal numbers for injection.

In Vivo MSC Homing

C57BL/6 mice (Charles River Laboratories) were anesthetized with ketamine/xylazine and their ears shaved 24 hr prior to cell infusion. To induce an inflammatory response, 30 μg of *E. coli* lipopolysaccharide in 50 μl saline was injected into the pinna of the left ear, with 50 μl 0.9% saline injected into the right ear as a control. To evaluate the impact of Ro-31-8425 pretreatment on MSC homing to the inflamed ear, MSCs were incubated in cell culture media with 3 μM Ro-31-8425 (dissolved in 0.1% DMSO) or 0.1% DMSO vehicle alone as a control for 24 hr before staining and in vivo administration. Cells were stained prior to infusion as described above. For Ab blocking experiments, pretreated or control MSCs were washed and incubated for 30 min with mouse anti-human CD11a (clone TS1/22) or mouse IgG1 isotype control, followed by two washing steps in PBS prior to staining with the Vybrant dyes. After staining, 4×10^4 cells of each condition were suspended in 150 μl PBS (pH 7.4) and injected by retro-orbital vein infusion into each mouse, so that each mouse received vehicle treated-MSCs of one color and Ro-31-8425 pretreated-MSCs of another. The stain color pair was switched between mice to correct for detection sensitivity. To highlight the vasculature, FITC-dextran (2×10^6 kDa) was injected retro-orbitally prior to imaging. Studies were in accordance with U.S. NIH guidelines for care and use of animals under approval of the institutional animal care and use committees of Massachusetts General Hospital and Harvard Medical School.

Confocal Fluorescence Microscopy

In vivo homing of MSCs to the skin was imaged (24 hr post-cell infusion) noninvasively in real time using a custom-built video-rate laser-scanning confocal microscope designed specifically for live-animal imaging as previously described (Mortensen et al., 2013). See also Supplemental Experimental Procedures.

Ear Thickness and TNF-α ELISA

To determine the impact of small-molecule pretreatment on MSC therapeutic potential, ear swelling was measured. As a baseline, we measured ear thickness of all mice to be used using a caliper (Mitutoyo) and found no difference. Each measurement was taken three times with the average value recorded, and care was taken to ensure minimal compression. Inflammation was then induced as described above. 24 hr later, mice (n = 4–8 per group) were infused with no MSCs, MSCs (10^6/20 g body weight) pretreated for 24 hr with 0.1% DMSO, or MSCs (10^6/20 g body weight) pretreated for 24 hr with 3 μM Ro-31-8425. 24 hr after cell infusion, ear thickness was measured using a caliper as before. To evaluate TNF-α secretion, LPS-induced inflammation and MSC administration were performed as described above with n = 4–6 mice for each condition. Mice were sacrificed 24 hr after cell administration, and both ears were harvested. Ears were then ground in ice-cold extraction buffer (RIPA with 0.5% Tween-20) using a homogenizer, homogenates were centrifuged at 13,000 × *g* for 10 min at 4°C, and the level of mouse TNF-α level in the supernatant samples was quantified using an anti-mouse TNF-α ELISA kit (BioLegend).

SUPPLEMENTAL INFORMATION

Supplemental Information includes Supplemental Experimental Procedures and three figures and can be found with this article online at http://dx.doi.org/10.1016/j.celrep.2015.01.057.

AUTHOR CONTRIBUTIONS

O.L. and L.J.M. co-wrote the paper, designed experiments, performed experiments, and analyzed and interpreted data. G.B., Z.T., C.P., B.B., and J.Z. designed experiments, performed experiments, and analyzed and interpreted data. T.S., E.H., H.S., J.M., and Z.Y. performed experiments and analyzed data. M.C., J.R., and J.F.D. designed experiments and interpreted data. C.P.L. and J.M.K. co-wrote the paper, designed experiments, and interpreted data.

ACKNOWLEDGMENTS

The authors wish to thank Sophie Fontaine and Céline Chansac from Sanofi for their technical support. This work was supported by a research grant from Sanofi-Aventis U.S. to J.M.K. and C.P.L. and by National Institutes of Health grants HL095722 (to J.M.K.) and P41 EB015903-02S1 (to C.P.L.). G.B., C.P., B.B., J.Z., M.C., and J.R. are employed by Sanofi. J.M.K. consults in the field of cell therapy for Stempeutics, Sanofi, and Mesoblast.

Received: March 25, 2014
Revised: December 14, 2014
Accepted: January 24, 2015
Published: February 26, 2015

REFERENCES

Ankrum, J., and Karp, J.M. (2010). Mesenchymal stem cell therapy: two steps forward, one step back. Trends Mol. Med. *16*, 203–209.

Ankrum, J.A., Ong, J.F., and Karp, J.M. (2014). Mesenchymal stem cells: immune evasive, not immune privileged. Nat. Biotechnol. *32*, 252–260.

Bhatia, S.K., King, M.R., and Hammer, D.A. (2003). The state diagram for cell adhesion mediated by two receptors. Biophys. J. *84*, 2671–2690.

Brehmer, D., Godl, K., Zech, B., Wissing, J., and Daub, H. (2004). Proteome-wide identification of cellular targets affected by bisindolylmaleimide-type protein kinase C inhibitors. Mol. Cell. Proteomics *3*, 490–500.

Cutler, C., Multani, P., Robbins, D., Kim, H.T., Le, T., Hoggatt, J., Pelus, L.M., Desponts, C., Chen, Y.B., Rezner, B., et al. (2013). Prostaglandin-modulated umbilical cord blood hematopoietic stem cell transplantation. Blood *122*, 3074–3081.

de Girolamo, L., Lucarelli, E., Alessandri, G., Avanzini, M.A., Bernardo, M.E., Biagi, E., Brini, A.T., D'Amico, G., Fagioli, F., Ferrero, I., et al.; Italian Mesenchymal Stem Cell Group (2013). Mesenchymal stem/stromal cells: a new "cells as drugs" paradigm. Efficacy and critical aspects in cell therapy. Curr. Pharm. Des. *19*, 2459–2473.

Dominici, M., Le Blanc, K., Mueller, I., Slaper-Cortenbach, I., Marini, F., Krause, D., Deans, R., Keating, A., Prockop, Dj., and Horwitz, E. (2006). Minimal criteria for defining multipotent mesenchymal stromal cells. The International Society for Cellular Therapy position statement. Cytotherapy *8*, 315–317.

Enoki, C., Otani, H., Sato, D., Okada, T., Hattori, R., and Imamura, H. (2010). Enhanced mesenchymal cell engraftment by IGF-1 improves left ventricular function in rats undergoing myocardial infarction. Int. J. Cardiol. *138*, 9–18.

François, M., and Galipeau, J. (2012). New insights on translational development of mesenchymal stromal cells for suppressor therapy. J. Cell. Physiol. *227*, 3535–3538.

Hoogduijn, M.J., Popp, F., Verbeek, R., Masoodi, M., Nicolaou, A., Baan, C., and Dahlke, M.H. (2010). The immunomodulatory properties of mesenchymal stem cells and their use for immunotherapy. Int. Immunopharmacol. *10*, 1496–1500.

Joy, S.V., Scates, A.C., Bearelly, S., Dar, M., Taulien, C.A., Goebel, J.A., and Cooney, M.J. (2005). Ruboxistaurin, a protein kinase C beta inhibitor, as an emerging treatment for diabetes microvascular complications. Ann. Pharmacother. *39*, 1693–1699.

Karp, J.M., and Leng Teo, G.S. (2009). Mesenchymal stem cell homing: the devil is in the details. Cell Stem Cell *4*, 206–216.

Kim, I., Moon, S.O., Kim, S.H., Kim, H.J., Koh, Y.S., and Koh, G.Y. (2001). Vascular endothelial growth factor expression of intercellular adhesion molecule 1 (ICAM-1), vascular cell adhesion molecule 1 (VCAM-1), and E-selectin through nuclear factor-kappa B activation in endothelial cells. J. Biol. Chem. *276*, 7614–7620.

Ko, I.K., Kim, B.G., Awadallah, A., Mikulan, J., Lin, P., Letterio, J.J., and Dennis, J.E. (2010). Targeting improves MSC treatment of inflammatory bowel disease. Mol. Ther. *18*, 1365–1372.

Kumar, S., and Ponnazhagan, S. (2007). Bone homing of mesenchymal stem cells by ectopic alpha 4 integrin expression. FASEB J. *21*, 3917–3927.

Levy, O., Anandakumaran, P., Ngai, J., Karnik, R., and Karp, J.M. (2013a). Systematic analysis of in vitro cell rolling using a multi-well plate microfluidic system. J. Vis. Exp. *80*, e50866.

Levy, O., Zhao, W., Mortensen, L.J., Leblanc, S., Tsang, K., Fu, M., Phillips, J.A., Sagar, V., Anandakumaran, P., Ngai, J., et al. (2013b). mRNA-engineered mesenchymal stem cells for targeted delivery of interleukin-10 to sites of inflammation. Blood *122*, e23–e32.

Luster, A.D., Alon, R., and von Andrian, U.H. (2005). Immune cell migration in inflammation: present and future therapeutic targets. Nat. Immunol. *6*, 1182–1190.

Mortensen, L.J., Levy, O., Phillips, J.P., Stratton, T., Triana, B., Ruiz, J.P., Gu, F., Karp, J.M., and Lin, C.P. (2013). Quantification of Mesenchymal Stem Cell (MSC) delivery to a target site using in vivo confocal microscopy. PLoS ONE *8*, e78145.

Muid, R.E., Dale, M.M., Davis, P.D., Elliott, L.H., Hill, C.H., Kumar, H., Lawton, G., Twomey, B.M., Wadsworth, J., Wilkinson, S.E., et al. (1991). A novel conformationally restricted protein kinase C inhibitor, Ro 31-8425, inhibits human neutrophil superoxide generation by soluble, particulate and post-receptor stimuli. FEBS Lett. *293*, 169–172.

Newell, E.W., Sigal, N., Nair, N., Kidd, B.A., Greenberg, H.B., and Davis, M.M. (2013). Combinatorial tetramer staining and mass cytometry analysis facilitate T-cell epitope mapping and characterization. Nat. Biotechnol. *31*, 623–629.

Prockop, D.J., and Oh, J.Y. (2012). Medical therapies with adult stem/progenitor cells (MSCs): a backward journey from dramatic results in vivo to the cellular and molecular explanations. J. Cell. Biochem. *113*, 1460–1469.

Rombouts, W.J., and Ploemacher, R.E. (2003). Primary murine MSC show highly efficient homing to the bone marrow but lose homing ability following culture. Leukemia *17*, 160–170.

Sackstein, R., Merzaban, J.S., Cain, D.W., Dagia, N.M., Spencer, J.A., Lin, C.P., and Wohlgemuth, R. (2008). Ex vivo glycan engineering of CD44 programs human multipotent mesenchymal stromal cell trafficking to bone. Nat. Med. *14*, 181–187.

Sarkar, D., Spencer, J.A., Phillips, J.A., Zhao, W., Schafer, S., Spelke, D.P., Mortensen, L.J., Ruiz, J.P., Vemula, P.K., Sridharan, R., et al. (2011). Engineered cell homing. Blood *118*, e184–e191.

Song, B.W., Chang, W., Hong, B.K., Kim, I.K., Cha, M.J., Lim, S., Choi, E.J., Ham, O., Lee, S.Y., Lee, C.Y., et al. (2013). Protein kinase C activation stimulates mesenchymal stem cell adhesion through activation of focal adhesion kinase. Cell Transplant. *22*, 797–809.

Tang, S., Xiao, V., Wei, L., Whiteside, C.I., and Kotra, L.P. (2008). Protein kinase C isozymes and their selectivity towards ruboxistaurin. Proteins *72*, 447–460.

Teo, G.S., Ankrum, J.A., Martinelli, R., Boetto, S.E., Simms, K., Sciuto, T.E., Dvorak, A.M., Karp, J.M., and Carman, C.V. (2012). Mesenchymal stem cells transmigrate between and directly through tumor necrosis factor-α-activated endothelial cells via both leukocyte-like and novel mechanisms. Stem Cells *30*, 2472–2486.

Tong, Z., Duncan, R.L., and Jia, X. (2013). Modulating the behaviors of mesenchymal stem cells via the combination of high-frequency vibratory stimulations and fibrous scaffolds. Tissue Eng. Part A *19*, 1862–1878.

Wong, D., and Dorovini-Zis, K. (1992). Upregulation of intercellular adhesion molecule-1 (ICAM-1) expression in primary cultures of human brain microvessel endothelial cells by cytokines and lipopolysaccharide. J. Neuroimmunol. *39*, 11–21.